Tricontinuous Double Gyroid Cubic Phase in Triblock Copolymers of the ABA Type

Apostolos Avgeropoulos,[†] Benita J. Dair,[‡] Nikos Hadjichristidis,*[,†] and Edwin L. Thomas*[,‡]

Department of Chemistry, University of Athens, Panepistimiopolis, 157 71 Zografou, Athens, Greece, and Department of Materials Science, Massachusetts Institute of Technology, Cambridge, Massachusetts 02139

Received February 27, 1997; Revised Manuscript Received June 9, 1997[⊗]

ABSTRACT: We report the synthesis and morphological characterization of two triblock copolymers of the ABA type, where A is polystyrene (PS) and B polyisoprene (PI). The volume fraction of the minority component, PS or PI, is approximately 1/3. Cubic microdomain morphologies, already found in diblock and star block copolymers with the same composition range, are observed for the first time in the case of linear triblock copolymers. The two ABA triblocks are on opposite sides of the phase diagram, which signifies that both the A end blocks and the B midblock are capable of forming the interconnected double network structure. Investigation of the morphology was done via birefringence, small-angle X-ray scattering (SAXS), and transmission electron microscopy (TEM). Birefringence measurements showed each triblock structure to have isotropic optical properties. The characteristic ratio of the observed Bragg peaks, q_2/q_1, was approximately $\sqrt{4}/\sqrt{3}$ for each sample, indicating a set of eight possible cubic space groups. TEM data showed an interconnected tricontinuous microdomain structure. Since the two triblocks have essentially complementary structures (PS = 0.32 in one and PI = 0.36 in the other), the TEM images of OsO_4-stained thin sections are complementary and the diffraction patterns of the images are approximately equal according to Babinet's principle. Examination of high-symmetry projections demonstrated *p*6*mm*, *p*4*mm*, and *c*2*mm* symmetry present in the TEM images. Comparison with the ⟨111⟩, ⟨100⟩, and ⟨110⟩ projections of the eight cubic space groups satisfying the SAXS data eliminated all but the $Fm\bar{3}m$ and $Ia\bar{3}d$ groups as possible structures. Due to the observed connectivity of the structure, the $Fm\bar{3}m$ structure could be eliminated by inspection of possible network structures and the resultant symmetries. Computer simulations of a model structure (double gyroid) based on level surfaces with $Ia\bar{3}d$ symmetry and their Fourier transforms showed excellent agreement with the high-symmetry projections and their respective optical transforms.

Introduction

In this work we demonstrate that the double gyroid structure appears in the case of linear triblock copolymers in a composition range 0.32−0.36 independent of whether the minority components are the end blocks or the midblock. Thus, both the A end blocks and the B midblock of an ABA triblock are capable of forming the interconnected double networks. Additionally, we emphasize the appropriate characterization strategy that enables distinction between the DG and other interconnected cubic structures using a combination of birefringence, SAXS, and quantitative TEM measurements.

We begin with a survey of the appearance of the two interconnected cubic morphologies found in various block copolymer systems. In 1976, Aggarwal showed a TEM image of an interconnected, highly ordered microphase-separated structure without comment about the precise domain structure of the polystyrene (PS) and polyisoprene (PI) radial star block copolymer consisting of 30 weight % PS and having 15 arms.[1] Fetters and Thomas[2,3] undertook a detailed study of the morphology of star diblock copolymers, and in 1986, the ordered bicontinuous double diamond (OBDD) cubic morphology was reported as a new equilibrium microdomain structure in star block copolymers of PS and PI with 8, 12, and 18 arms, for a minority PS volume fraction of 0.27.

The ordered bicontinuous double diamond structure consists of two interpenetrating but nonintersecting networks of the minority component in a matrix of the majority. The reader should keep in mind that at least some of the structures initially identified as OBDD (space group $Pn\bar{3}m$) may actually be double gyroid (space group $Ia\bar{3}d$) (see later discussion). In the OBDD structure, each network exhibits the symmetry of a diamond cubic lattice with each node displaying tetrahedral symmetry. Both the networks and the matrix are three-dimensionally continuous. The interface between the two components can be represented by a topologically connected intermaterial dividing surface (IMDS),[4] and the structure exhibits $Pn\bar{3}m$ space group symmetry. One striking characteristic of this OBDD morphology was the "wagon-wheel" like patterns frequently observed in the TEM images. Indeed, the published micrograph in Aggarwal's review was very similar to the characteristic [111] projection of the OBDD, suggesting that the original radial arm copolymer exhibited this structure. In another study[5] of star block copolymers with PS volume fraction of 0.27, the Thomas group found that a structural transition occurred from hexagonally packed cylinders to OBDD in star block copolymers depending on the number of arms. For stars with 2 (a 2-arm star is an ABA triblock), 4, or 5 arms, the morphology was hexagonally packed cylinders, while star blocks with 6, 8, 12, or 18 arms displayed an OBDD structure.

An extensive study[6] of 18-arm star block copolymers of PS and PI extended results to other compositions and showed that the OBDD structure appears not only for a PS outer block star copolymer with a composition of 0.27 and 0.32 volume fraction PS but also for the case

* To whom correspondence should be addressed.
† University of Athens.
‡ Massachusetts Institute of Technology.
⊗ Abstract published in *Advance ACS Abstracts,* September 1, 1997.

S0024-9297(97)00266-0 CCC: $14.00

when PI is the outer minority block, with a composition of 0.27 volume fraction PI.

The Hashimoto group[7] observed the new morphology in linear diblock copolymers in the range between 0.62 and 0.66 for PS content. They reported that this novel structure appears only on one side of the phase diagram and described the basic unit of the minority component as a tetrapod composed of four short rodlike elements of the PI phase. These units are linked to form ordered, 3-dimensional networks with the PS block filling the matrix. Hashimoto et al. suggested this tetrapod network structure is most likely the OBDD structure of the star blocks described above. This morphology also appeared in a tricomponent pentablock copolymer of the I−S−I−A−I type (I is polyisoprene, S is polystyrene, and A is poly[(4-vinylbenzyl)dimethylamine]), where a single diamond lattice (space group symmetry $Fd\bar{3}m$) was considered as a possible model for the bicontinuous structure.[8]

It should also be mentioned that structures having $Pn\bar{3}m$ symmetry were observed in the past in liquid crystal and surfactant systems.[9,10]

Evidence of the OBDD morphology was also obtained in binary blends of an initially lamellar poly(styrene-*b*-isoprene) diblock copolymer and homopolymer polystyrene (hPS) of various molecular weights.[11] The microdomain size could be altered by changing the molecular weight of the homopolymer. The mean curvature of the IMDS and the area per junction increase when the hPS concentration is increased and/or when the molecular weight of the hPS is decreased. The OBDD structure in the binary blends[12] occurred for an overall PS volume fraction equivalent to that for the neat copolymers, namely 0.64−0.67. The dependence of this cubic structure on the diblock molecular weight in the blends was also studied.[13] It should be pointed out that if the pure diblock forms the lamellar morphology, then in the blend the hPS resides in the matrix of the OBDD. If instead the pure diblock forms the cylindrical morphology, then the hPS resides inside the network region. Attempts to obtain the OBDD blend morphology with hPS in the matrix by using a diblock with cylindrical microdomains failed.

Results from a transmission electron microscopy study of linear triblock copolymer/homopolymer blends,[14] composed of a poly(styrene-*b*-butadiene-*b*-styrene) triblock (forming cylinders itself) and poly(vinyl methyl ether) homopolymer, showed that this system exhibited the OBDD morphology as well. The homopolymer PVME and the PS blocks of the copolymers mix together in the channels, while the PBd blocks of the copolymer occupy the matrix region. This cubic structure, generated in copolymer/homopolymer blends with total hard phase volume fraction equal to 0.3, was the first made using a triblock copolymer.

Mogi et al.[15,16] found an ordered tricontinuous double-diamond (OTDD) structure during their study of the morphology of triblock copolymers of the ABC type, where A is PI, B is PS, and C is poly(2-vinylpyridine) (PVP). The OTDD is similar to the OBDD structure for diblock copolymers, the difference being that in the OTDD case there are the two chemically distinct minority component networks formed by the two end blocks. In the TEM study of these samples[15] images from two different projections of the structure (the [111] and the [001]) were shown. The volume fraction of PS at which OTDD was observed was between 0.48 and 0.66. Earlier work in such ABC triblocks has shown the existence of these peculiar and complex structures, but no further explanations were given,[17−20] not only because the preparation of well-characterized samples was difficult but also because the equilibrium morphologies were not systematically studied.

The Noda group[21,22] also found the OTDD structure in styrene−isoprene−2-vinylpyridine triblock copolymers of the ABC type, which consist of the same components as in ref 15 and 16, but with a different block sequence. It was supposed that these triblocks would form symmetric equilibrium morphologies, when the A and C blocks have the same volume fraction and when A/B and B/C interfaces possess similar surface energies. Although the TEM image showed a clear bicontinuous morphology, the SAXS patterns exhibited broad shoulders and weak peaks, making indexing for the OTDD structure somewhat speculative.

During a study by Gobran[23] of diblock copolymer thermal behavior, an unusual microphase order−order transition was noted in a low molecular weight polystyrene−polyisoprene diblock copolymer containing 34% PS. The sample formed a lamellar phase under normal casting and annealing (120 °C) conditions, but when annealed at higher temperatures, the characteristic diffraction for lamellae disappeared and new peaks appeared with the two prominent low-order reflections having $q_2/q_1 \approx \sqrt{4}/\sqrt{3}$. TEM results of samples quenched from the high-temperature phase revealed that the new morphology was three-dimensionally continuous and consisted of interpenetrating styrene and isoprene domains similar to those for the OBDD.[23,24] However, a definitive structural assignment could not be made due to the limited quality of the TEM and SAXS data resulting from the restricted long range order of the microdomain morphology.

Subsequently, by combining high-resolution SAXS, computer simulations, and TEM of well-annealed specimens, the equilibrium high-temperature microphase was shown to be a bicontinuous cubic phase, but *not* the OBDD.[25] SAXS data from the new structure were most consistent with space group $Ia\bar{3}d$. TEM images showed clear 6-fold and 4-fold patterns quite similar to previously published images of the OBDD. However, simulated projections of a constant thickness model based on the gyroid minimal surface showed excellent agreement with the TEM data. This structure was initially termed gyroid*, with the symbol "*" used to distinguish the morphology from the G (for gyroid) minimal surface.[26] The structure consists of two interpenetrating but nonintersecting networks (as in the OBDD) of the minority component in a matrix of the majority. The networks are three-dimensionally continuous and enantiomeric, with nodes having trigonal symmetry. Due to the similarity to the double diamond structure, and admitting to the future possibility of the discovery of a single network structure (possibly already found, see ref 8), we now prefer to call the interconnected network structure with $Ia\bar{3}d$ symmetry the double gyroid (DG). Simultaneously, Bates and coworkers using SAXS and TEM discovered an $Ia\bar{3}d$ morphology in a 60/40 binary copolymer blend[27] consisting of two intermediate segregated SI diblock copolymers of equal molecular weights but different compositions and in a shear-oriented polystyrene−poly(2-vinylpyridine) diblock copolymer.[28]

In spite of the difference in symmetry between the two interconnected-minority-block-network cubic phases, computer simulations of TEM images based on a paral-

lel surface construct employing the G minimal surface as the base surface indicated that certain projections of the gyroid* (DG henceforth) resembled those for the OBDD (DD henceforth) morphology. In particular, when viewed along the [111] direction, both the DG and the DD structures can produce the "wagon wheel"[29] projection depending on the slice thickness.[30] This, plus the fact that the ratios q_2/q_1 of the first two allowed reflections for each of the space groups were reasonably close (for DD the ratio is $\sqrt{3}/\sqrt{2} = 1.225$, whereas for DG the ratio is $\sqrt{4}/\sqrt{3} = 1.155$) prompted a careful reexamination[31] of two polystyrene−polyisoprene star block copolymer samples previously thought to possess the DD morphology.[2−4] By employing an improved SAXS apparatus and longer annealing procedures, the scattering patterns showed four reflections for both star block samples. After comparing the predicted and measured peak positions and intensities for a 0.27 volume fraction minority component for the constant thickness models of the DD and the DG structures, the conclusion was that the scattering results are most consistent with the $Ia\bar{3}d$ space group. After this study it was suggested that other copolymer and copolymer/homopolymer blend systems whose structures were previously identified only by TEM using the "wagon wheel" image as the characteristic signature of the OBDD may in fact have microdomain structures more consistent with the DG phase.

A recent study[32] of the morphologies of miktoarm block copolymers with architectures of the type $(PS_{aM}-PI_M)_n-(PS_M-PI_{aM})_n$, where M = 20K, n = 1,2, and the arm asymmetry parameter a = 1, 2, or 4 (a is the ratio of the outer block molecular weight to that of the inner block), showed the DD structure for a star block with n = 2 and a = 4. TEM images exhibiting 6- and 4-fold symmetry and a continuous PS and PI microdomain geometry, together with optical measurements of approximately zero birefringence, suggested an interconnected cubic structure. SAXS data were inconclusive due to the insufficient peak resolution for this high molecular weight (400 000) star copolymer. However, excellent matches of the TEM data with level surface models based on the DD structure were found for the [110] projection (which can be used to differentiate between the DD and DG structures), whereas matches to the DG structure were poor.[33] Thus, it is quite important to be able to distinguish DD from DG using TEM data as well as SAXS data.

Experimental Methods

Both triblocks were prepared by anionic polymerization using high-vacuum techniques in evacuated, *n*-BuLi-washed, benzene-rinsed glass vessels. The purification of styrene (Merck), isoprene (Fluka), and benzene (Merck) to the standards required for anionic polymerization have been described elsewhere.[34−36] Tetrahydrofuran (THF, Merck) was stirred overnight over CaH_2, distilled on the vacuum line to a sodium mirror, and left to react for 24 h. This procedure was repeated until no degradation of the mirror was observed. Then it was distilled into a flask containing a sodium mirror and traces of styrene. The appearance of a red color due to the formation of polystyrylsodium (PSNa) indicated the high purity of the THF. A middle fraction of THF was used. Dichlorodimethylsilane was fractionally distilled on the vacuum line and was subdivided into ampules. *s*-BuLi, prepared from *sec*-butyl chloride and a lithium dispersion, was the initiator and C_6H_6 the solvent for all polymerizations.

Fractionation was carried out by adding methanol to the stirred polymer solution (∼0.5% w/v) in toluene at room temperature until turbidity was detected. The mixture was then heated and stirred gently until clear, transferred to a warm separatory funnel and allowed to equilibrate to room temperature overnight. This procedure was repeated until no precursors or undesirable products were shown to be present by size exclusion chromatography (SEC).

SEC experiments were carried out at 30 °C using a Waters model 510 pump, Waters Model 410 differential refractometer, and Waters model 486 tunable absorbance detector. Three Phenomenex (type, phenogel 5 linear; pore size, 50−10^6 Å) columns were used. THF, distilled over CaH_2 and sodium, was the carrier solvent at a flow rate of 1 mL/min.

The weight-average molecular weight (M_w) of the final polymers was determined with a Chromatix KMX-6 low-angle laser photometer (LALLS). This instrument, equipped with a helium−neon laser, was operated at a wavelength of 633 nm. The refractive index increments, dn/dc in THF at 25 °C, were measured with a Chromatix KMX-16 refractometer.

The number-average molecular weight (M_n) was determined with a Wescan Model 230 membrane osmometer at 35 °C. Toluene, distilled over CaH_2, was the solvent.

The M_w values were obtained from the $(KC/\Delta R_\theta)^{1/2}$ vs C plots (ΔR_θ, excess Rayleigh ratio; K, combination of known optical constants; C, concentration) and the M_n values from the $(\Pi/C)^{1/2}$ vs C plots (Π is the osmotic pressure). In all cases the correlation coefficient was better than 0.99.

^{1}H-NMR determination of the composition and the microstructure of the materials was carried out in $CDCl_3$ at 30 °C using a Varian Unity Plus 300/54 instrument. For the polyisoprene block, the typical microstructure characteristic of anionic polymerization of isoprene in benzene was observed (9 wt % 3,4, 70 wt % *cis*-1,4, and 21 wt % *trans*-1,4).

More details concerning the SEC, MO, LALLS, and NMR measurements are given elsewhere.[35,36]

Polymer degradation after the annealing procedures was checked by dissolving a portion of each of the annealed samples in THF and rerunning SEC. No detectable difference was observed, indicating no unreacted linking agent left after the fractionation procedure and no high-temperature branching of PI.

For SAXS and TEM characterization, approximately 0.7 mm thick films of the materials were cast from a dilute solution (∼4 wt %) with a nonselective solvent (toluene) over a period of 1 week at ambient conditions. Then the polymer films were dried for 2 days under vacuum at room temperature. The PI-rich triblock film was subsequently annealed at 120 °C for 10 days under vacuum, and the PS-rich triblock film was annealed at 130 °C and 8 days under vacuum.

The X-ray diffraction (SAXS) data were acquired at the Time-Resolved Diffraction Facility (station X12B) at the National Synchrotron Light Source at Brookhaven National Laboratory (BNL) using a custom-built two-dimensional detector (10 × 10 cm, 512 × 512 pixels).[37] The optical system provides a doubly-focused (spot size, 0.5 × 0.5 mm fwhm) monochromatic X-ray beam (bandpass, $\sim 5 \times 10^{-4}$ $\Delta\lambda/\lambda$) with a wavelength of λ = 1.54 Å.

SAXS data are represented by plots of scattered intensity as a function of the scattering vector **q**, which is defined as

$$\mathbf{q} = \frac{4\pi \sin\theta}{\lambda} \tag{1}$$

where θ is half of the scattering angle 2θ and λ is the wavelength of the X-rays.

Using this relation and Bragg's law for scattering,

$$\lambda = 2d_{hkl} \sin\theta \tag{2}$$

the d spacing of the scattering hkl planes are related to the scattering vector by the following equation:

$$d_{hkl} = \frac{2\pi}{q_{hkl}} \tag{3}$$

For TEM investigation, 500−1500 Å thick sections were cryomicrotomed at approximately −90 °C using a Reichert-Jung FC 4E cryoultramicrotome equipped with a diamond

knife. Although the section thicknesses varied between 500 and 1500 Å, only the thinnest sections (500−1000 Å thick) were used for the images and their subsequent optical transforms. The thickness of the high-symmetry projection grains was determined by spraying two different sizes of PS spheres, one size on each side of the section using an atomizer. From images taken before and after a known amount of specimen tilt, measurement of the relative separation distance of a pair of different size spheres permits calculation of the average sample thickness. Sections were picked up on 600-mesh copper grids and then placed in the vapors of a 4% osmium tetroxide−water solution for 2 h for selective staining of the polyisoprene phase. A JEOL 200CX electron microscope, operated at 200 kV in the bright field mode, was used to examine the stained sections. Images of high symmetry were obtained using a goniometer stage with ±45° tilt capability on the *x*-axis and ±27° on the *y*-axis (double tilt holder).

The double tilt holder in the TEM allows selection of grains of the required orientation. Optical transforms of the TEM negatives were taken with a custom-built optical diffractometer using a 5 mW polarized UniPhase helium−neon laser with $\lambda = 633$ nm. The diffractometer was equipped with a camera shutter, and diffraction patterns were recorded using Polaroid film. The diffraction patterns (optical transforms) of high symmetry areas were in most cases very clear, exhibiting up to third-order peaks and were qualitatively comparable with those obtained from FFTs of appropriate computer-simulated projections. Several different exposures were required of the optical transforms in order to capture and observe different order diffraction peaks due to the limited dynamic range of the film.

Level surface models are convenient to model 3D periodic, interconnected microphase-separated structures.[38] The level surfaces we employ are simple trigonometric functions that maintain the symmetries of a given space group. Families of level surfaces $F(x,y,z)$ can be constructed by variation of the constant, $t = F(x,y,z)$. While level surfaces do not have constant mean curvature nor constant thickness, they can provide *connected* surfaces of appropriate symmetry and volume fraction. To construct a level surface we use the lowest order allowed Fourier component of a space group and chose a particular value of the constant t that controls the volume fraction contained within the connected network. For the structures of interest here we use the following equation (G, space group $I4_132$, {110} Fourier component):

$$\text{single G:}\quad \sin x \cos y + \sin y \cos z + \sin z \cos x = t \qquad (4)$$

By taking *pairs* of surfaces $F(x,y,z) = \pm t$ the double gyroid structure with super group $Ia\bar{3}d$ is realized. Of course, a single gyroid structure can also be modeled. Simulations for different unit cell orientations, sample thicknesses, and slice locations within the unit cell were done on a Silicon Graphics Indigo 2 using the software TEMsim developed by J. Hoffman.[39] The simulations are based on the ray-tracing technique in which a ray-tracing algorithm is used for making 2-dimensional projections from 3-dimensional models of the candidate geometries described by intermaterial dividing surfaces.[40] For example, in order to mathematically describe the IMDS of the DG structure, which is composed of 2 triply periodic, tricontinuous networks embedded in a matrix, space was divided into three continuous regions by taking pairs of level surfaces. Each network has a volume fraction equal to half of the total minority volume fraction, and the matrix has the volume fraction of the majority component. The matrix was modeled to yield the desired majority volume fraction, which was 0.64 for the PS-rich sample and 0.68 for the PI-rich triblock. For DG surfaces, $t = \pm 1.0$ sufficed for both polymers, corresponding to a volume fraction of 0.66. Once a level surface was generated, it was sliced to a desired thickness defined by two parallel planes (*hkl*) oriented normal to a direction specified by the Miller indices [*hkl*]. Finally, the two-dimensional projection along [*hkl*] was made using the ray-tracing algorithm. This procedure is identical to microtoming a sample and examining it using TEM.

Fast Fourier transforms (FFTs) were made from the simulated TEM images. Approximately 32 × 32 unit cells were montaged together in a 1024 × 1024 pixel array. A program written by Dr. Robert Lescanec uses the 1024 × 1024 square input, multiplies it by a hanning window to reduce edge effects, performs the fast Fourier transform, and outputs the data on a log scale as a 2-dimensional image.[41]

Results and Discussion

Synthesis. The two triblock copolymers were synthesized using different approaches. The PS-rich triblock was synthesized by sequential addition of monomers, and the PI-rich copolymer, by linking half of the total triblock living PSPILi with $Cl_2Si(CH_3)_2$. The reactions used in each case are the following:

(a) Synthesis of the PS-rich triblock by sequential addition of monomers.

$$\text{St} + s\text{-BuLi} \xrightarrow{C_6H_6} (\text{PS})\text{Li} \qquad (\text{A})$$

$$(\text{PS})\text{Li} + \text{Is} \xrightarrow{C_6H_6} (\text{PS})(\text{PI})\text{Li} \qquad (\text{AB})$$

$$\xrightarrow[\text{of THF}]{\text{small amount}} \underset{\substack{\text{triblock copolymer}\\ \text{of the ABA type}}}{(\text{PS})(\text{PI})(\text{PS})}$$

(b) Synthesis of the PI-rich triblock by linking.

$$\text{St} + s\text{-BuLi} \xrightarrow{C_6H_6} (\text{PS})\text{Li} \qquad (\text{A})$$

$$(\text{PS})\text{Li} + \text{Is} \xrightarrow{C_6H_6} (\text{PS})(\text{PI})\text{Li} \qquad (\text{AB})$$

$$\text{(small excess)}\ (\text{PS})(\text{PI})\text{Li} + (CH_3)_2SiCl_2 \xrightarrow{C_6H_6} \underset{\substack{\text{triblock copolymer}\\ \text{of the ABA type}}}{[(\text{PS})(\text{PI})]_2Si(CH_3)_2} + (\text{PS})(\text{PI})\text{Li}$$

The major advantage of the sequential addition of monomers is that the final triblock is produced in 3 days and no fractionation is needed. In order to increase the initiation rate of the styrene toward the (PI)Li macroinitiator, a small amount of THF (less than 0.5 mL) was added. No change in the microstructure of the PI block occurs from the small amount of THF used, since THF is added after the complete polymerization of the isoprene. The only disadvantage of this method is that the two PS blocks may not have precisely the same molecular weight. In the case of the PS-rich triblock, the first PS block has $M_n = 19.5$K and the second $M_n = 20.5$K. This disadvantage is overcome by the chlorosilane (the second) approach. The use of chlorosilane leads to a final product having two end blocks with exactly the same molecular weight. However, the completion of the reaction needs at least 1 month in order to ensure that all the chlorosilane had reacted with the living diblock. The progress of the reaction was monitored by removing samples from the reactor and analyzing them by SEC. When there was no distinguishable change in the ratio of the two peaks, the triblock was purified from the diblock by fractionation. Typical SEC chromatograms of the precursors, the unfractionated and the fractionated triblock, are given in Figure 1a,b. The molecular characteristics of the two triblocks are shown in Table 1.

Structural Characterization. The structural symmetry of the triblocks was first studied through optical birefringence measurements. Materials exhibiting cubic

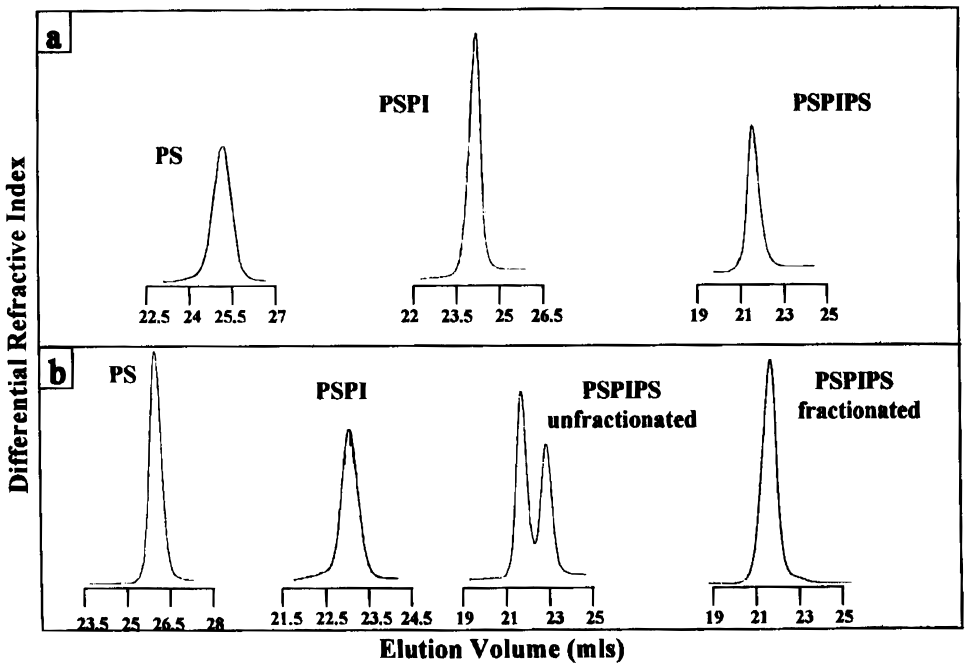

Figure 1. SEC chromatographs for (a) the PS-rich sample, prepared by sequential addition of monomers, and (b) the PI-rich sample, prepared by linking of the living diblock with Me_2SiCl_2.

Table 1. Molecular Characteristics of the Precursors and the Final Polymers

sample	10^{-3} M_n[a]	10^{-3} M_w[b]	I (SEC)	wt % PS (UV/SEC)	wt % PS (^{1}H-NMR)	wt % PS (calcd)
PS, 20K	19.5	20.0	1.03			
(PS)(PI), 20/20K	39.0	41.3	1.05	46	48	50
(PS)(PI)(PS) (PS-rich)	59.5	62.0	1.05	66	68	67
PS, 14K	13.3	14.1	1.05			
(PS)(PI), 14/24K	37.4	39.6	1.04	33	34	36
(PS)(PI)(PS) (PI-rich)	70.5	73.6	1.05	36	34	36

[a] From membrane osmometry (MO) in toluene at 35 °C. [b] From low-angle laser light scattering (LALLS) in THF at 25 °C.

symmetry show no birefringence because all second rank tensor properties (e.g., optical) of cubic crystals are isotropic. Noncubic periodic microphases are optically anisotropic and thus exhibit nonzero birefringences. Films of the triblocks showed negligible birefringence, indicating that the materials are either homogeneous or cubic. From the TEM images and SAXS patterns it can be seen that the two samples are microphase separated, so the factor of homogeneity must be excluded, leaving a cubic structure.

Selected bright-field TEM micrographs of the triblocks are shown in Figures 3a,e, 4a,c, and 5a,e. In both types of samples the grains exhibit 6-fold (Figure 3a,e), 4-fold (Figure 4a,c), and 2-fold (Figure 5a,e) symmetric projections, characteristic for a microphase with cubic symmetry. The TEM images suggest that both morphologies have interconnected structures; in the case of the PS-rich triblock, channels of PI and a matrix of PS are obtained and vice-versa for the PI-rich triblock.

Small-Angle X-ray Scattering. The scattering data plots for the two polymers are shown in Figure 2a,b. The PS-rich polymer displays only two distinct reflections, whereas the PI-rich polymer has several additional higher order peaks. The PS-rich SIS polymer with molecular weight of 20K/20K/20K was annealed at 130 °C for 8 days ($\chi N_{tot} \approx 55$), whereas the PI-rich SIS polymer with molecular weight 13.6K/46.4K/13.6K was annealed at 120°C for 14 days ($\chi N_{tot} \approx 80$).[42] Therefore it is not surprising that the PS-rich polymer is somewhat less ordered than the PI-rich sample.

The PS-rich polymer has a q_2/q_1 ratio of 1.156 ± 0.002, and the PI-rich polymer has a q_2/q_1 ratio of 1.162 ± 0.002. Considering the expected values of q_2/q_1 for various cubic space groups suggests $q_2/q_1 = \sqrt{4}/\sqrt{3} = \sqrt{8}/\sqrt{6}$; thus the first two reflections are either (111) and (200) or (211) and (220).

In both cases there are two prominent reflections with a characteristic $q_2/q_1 = 1.16$. Due to the lack of well-resolved reflections at larger q despite our annealing treatments, further distinction by SAXS would only be possible via laborious modeling of the intensity of the reflections using an appropriately defined IMDS and volume fraction for each space group. Instead, the approach we use in this paper is to eliminate candidate space groups by using observations from the experimental TEM images and considerations given to the geometrical requirements and implications of the observed interconnected structures.

There are eight possible cubic space groups consistent with the first two reflections in a ratio of $\sqrt{4}/\sqrt{3}$. These are $F23$, $Fm\bar{3}$, $Pa\bar{3}$, $F432$, $F\bar{4}3m$, $I\bar{4}3d$, $Fm\bar{3}m$, and $Ia\bar{3}d$. Further distinction among these can be made using the projected symmetries found from TEM images for the incident beam along the ⟨111⟩, ⟨100⟩, and ⟨110⟩ directions. The ⟨111⟩ experimental images of the two triblocks are shown in Figure 3a,e: both exhibit $p6mm$ symmetry. Of note is the wagon-wheel like structures found in this projection, which, as explained in the Introduction, has led to confusion in the past between the DD and DG morphologies. Parts a and c of Figure 4 show the ⟨100⟩ experimental images of the two triblocks: both exhibit $p4mm$ symmetry. Parts a and e of Figure 5 show the ⟨110⟩ experimental images, which

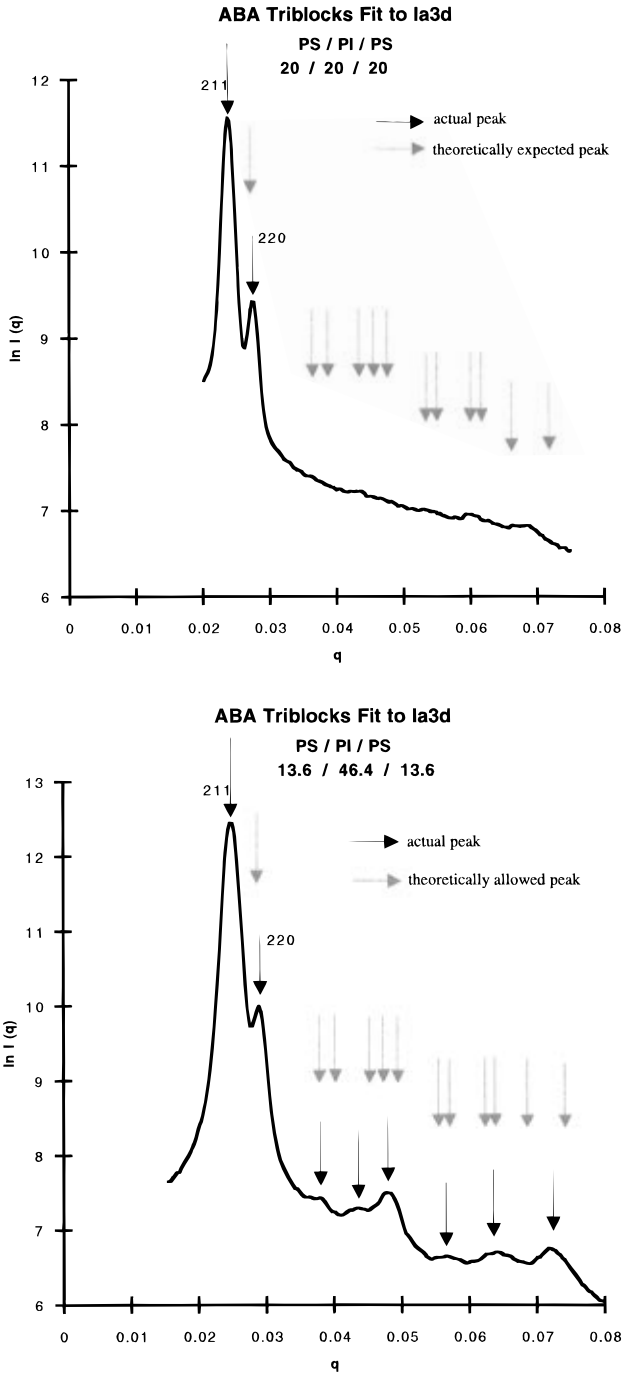

Figure 2. (a) ln $I(q)$ versus q plot for the PS-rich triblock, indexed to the $Ia\bar{3}d$ space group. Dark arrows represent actual peaks, while lighter arrows represent theoretically allowed peaks. (b) ln $I(q)$ versus q plot for the PI-rich triblock, indexed to the $Ia\bar{3}d$ space group.

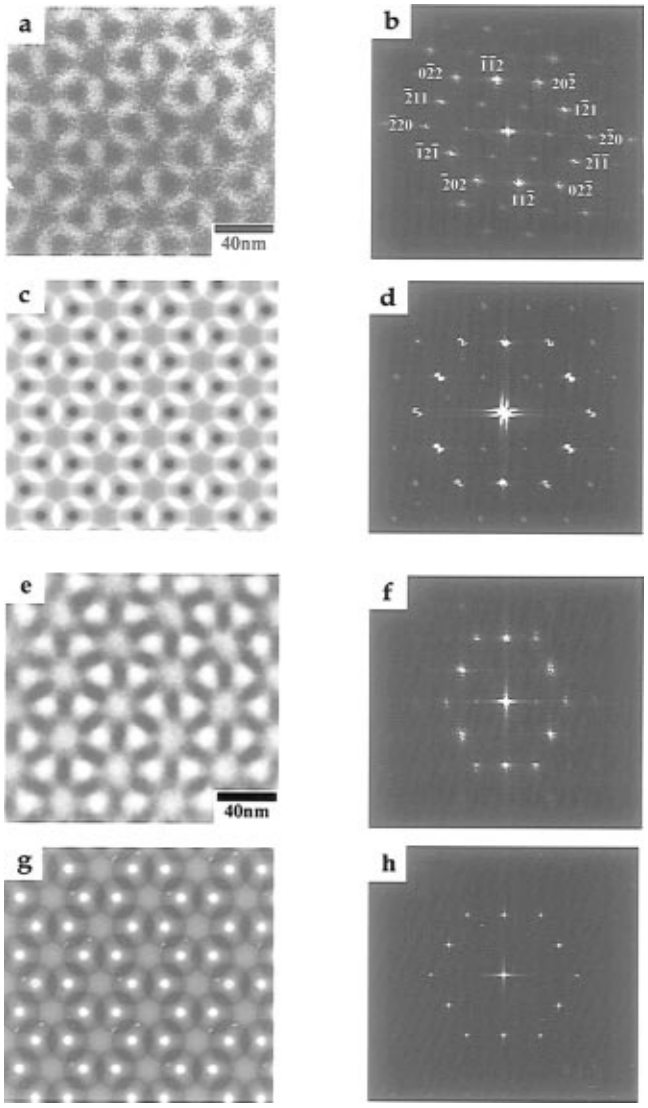

Figure 3. (a) Bright-field TEM image exhibiting the [111] projection of the PS-rich triblock. (b) FFT taken from the same image. (c) Simulated [111] projection of the G level surface, PS-rich; $t = \pm 1.0$; 1.0 unit cell thick. (d) FFT of the simulated G projection. (e) Bright-field TEM image exhibiting the [111] projection of the PI-rich triblock. (f) FFT taken from the same image. (g) Simulated [111] projection of the G level surface, PI-rich; $t = \pm 1.0$; 1.0 unit cell thick. (h) FFT of the simulated G projection.

both have $c2mm$ symmetry. Table 2 gives the set of eight possible cubic space groups consistent with the limited X-ray data and the plane group symmetry of their high-symmetry projections. By noting the symmetry observed in TEM images and their corresponding power spectra, we can eliminate certain of these space groups that fail to display the required symmetry of their high-symmetry projections. In this manner, the definite presence of the $p6mm$ symmetry for the ⟨111⟩ wagon wheel projection eliminates all but groups $Fm\bar{3}m$ and $Ia\bar{3}d$. Similarly, the clear occurrence of $p4mm$ symmetry for the ⟨100⟩ projection eliminates all but $F432$, $F\bar{4}3m$, $Fm\bar{3}m$, and $Ia\bar{3}d$. The $c2mm$ symmetry of the ⟨110⟩ images projection eliminates all but $Fm\bar{3}$, $F432$, $Fm\bar{3}m$, and $Ia\bar{3}d$. Taken together, SAXS and the high-symmetry TEM projections rule out six of the eight possible groups, leaving only $Fm\bar{3}m$ and $Ia\bar{3}d$.

A final constraint on the space group symmetry is the connectivity of the structure strongly suggested by the TEM data. Bicontinuous structures can be modeled using skeletal graphs. A skeletal graph is formed by joining nodes in a network by a series of straight segments.[26] The simplest trifunctional skeletal network known is that of the gyroid. A four-functional network can be made by using nodes with tetrahedral symmetry. A six-functional model is also possible. The trifunctional double gyroid structure with $Ia\bar{3}d$ symmetry satisfies all the constraints and appears as the best model. The nodes of a 3D network in the $Fm\bar{3}m$ structure cannot both be linked by trifunctional segments and retain the symmetry. Linking the nodes of $Fm\bar{3}m$ with tetrahedral functional segments results in a diamond structure, with change of the space group and subsequent loss of the q_2/q_1 ratio and required projections. Similarly, using

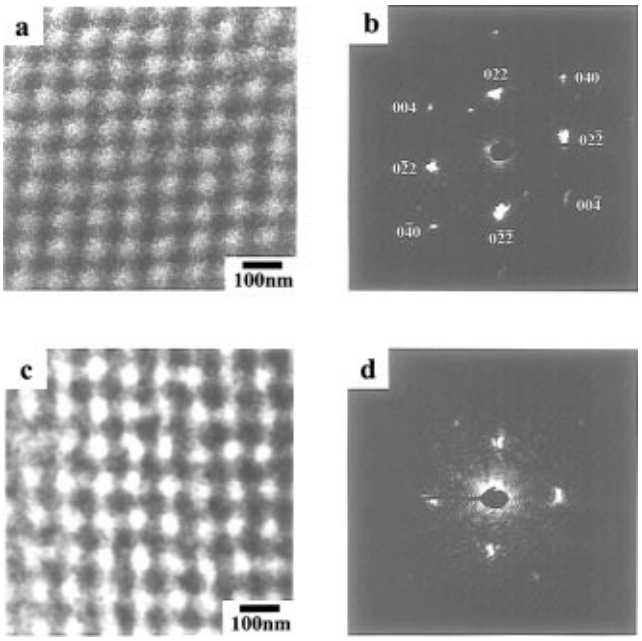

Figure 4. (a) Bright-field TEM image exhibiting the [001] projection of the PS-rich triblock. (b) Optical diffraction pattern taken from the [001] projection of the PS-rich triblock. (c) Bright-field TEM image exhibiting the [001] projection of the PI-rich triblock. (d) Optical diffraction pattern taken from the [001] projection of the PI-rich triblock.

hexafunctional nodes changes the structure to primitive cubic symmetry ($Pm\bar{3}m$) with likewise loss of the necessary SAXS peaks and high-symmetry TEM projections. Thus there is only one suitable space group left: $Ia\bar{3}d$.

Transmission Electron Microscopy. Selected bright-field TEM micrographs of the two triblocks are shown in Figures 3a,e (6-fold symmetric projections), 4a,c, (4-fold symmetric projections), and 5a,e (2-fold symmetric projections). Both samples exhibit the "wagon wheel pattern" (⟨111⟩ projection). As previously mentioned, wagon-wheel structures in the ⟨111⟩ projection have caused confusion in the morphological identification of block copolymers with cubic structures. Although SAXS results eliminate the $Pn\bar{3}m$ space group, it would be instructive to confirm that the morphology is double gyroid rather than double diamond.[43] An approach, which will be developed in a forthcoming paper,[44] is to perform a more quantitative evaluation of the TEM data on selected regions. Using the PS sphere-tilt method we determined the average section thickness for the PS-rich sample as 635 ± 10 Å and for the PI-rich sample as 710 ± 10 Å. Various candidate structures then can be distinguished by quantitative determination of the local section thickness and comparison of the images and optical diffraction patterns with the corresponding simulated projections and their fast Fourier transforms (FFT). However, for the purposes of this paper, since the space group of the DD structure has been eliminated, TEM will only be used to observe the nature of the interconnectivity of the structure, with TEMsim as a verification tool, to aid in the determination of the morphology.

Six-Fold Projection. Parts a and b of Figure 3 show the TEM image and its digitized Fourier transform (FFT) of the "wagon wheel" projection for the PS-rich triblock. Parts c and d of Figure 3 show the simulated TEM image and its FFT of a [111] projection of the DG structure, 1 unit cell thick, for the appropriate volume fraction. Parts e and h of Figure 3 compare the image and simulated projections and transforms for the [111] projection of the PI-rich triblock. The FFTs of the DG level surface models for both the PS- and PI-rich simulations each have 12 prominent peaks around the

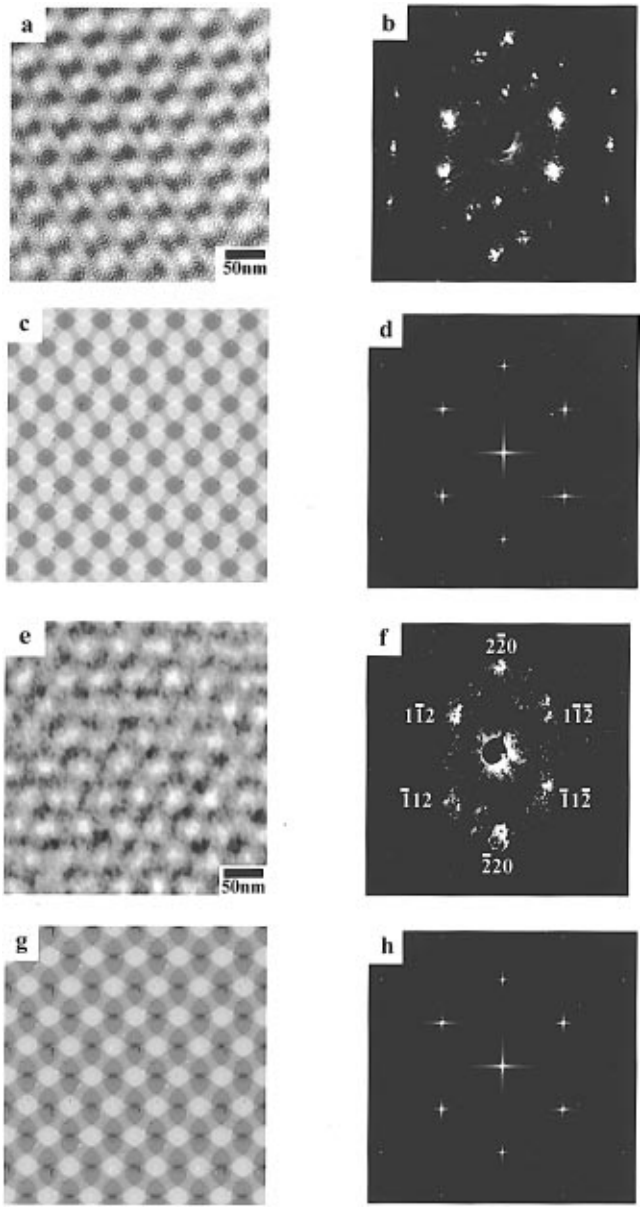

Figure 5. (a) Bright-field TEM image exhibiting the [110] projection of the PS-rich triblock. (b) Optical diffraction pattern taken from the same image. (c) Simulated [110] projection of the G level surface, PS-rich; $t = \pm 1.0$; 1.0 unit cell thick. (d) FFT of the simulated [110] projection of the G level surface. (e) Bright-field TEM image exhibiting the [110] projection of the PI-rich triblock. (f) Optical diffraction pattern taken from the same image. (g) Simulated [110] projection of the G level surface, PI-rich; $t = \pm 1.0$; 1.0 unit cell thick. (h) FFT of the simulated [110] projection of the G level surface.

Table 2. High-Symmetry Projections of Cubic Space Groups Having $q_2/q_1 = \sqrt{4}/\sqrt{3}$

space group	⟨111⟩	⟨100⟩	⟨110⟩
$F23$	$p3$	$p2mm$	$c1m1$
$Fm\bar{3}$	$p6$	$p2mm$	$c2mm$
$Pa\bar{3}$	$p6$	$p2gm$	$p2gg$
$F432$	$p3m1$	$p4mm$	$c2mm$
$F\bar{4}3m$	$p31m$	$p4mm$	$c1m1$
$I\bar{4}3d$	$p31m$	$p4gm$	$c1m1$
$Fm\bar{3}m$	$p6mm$	$p4mm$	$c2mm$
$Ia\bar{3}d$	$p6mm$	$p4mm$	$c2mm$

center beam, with an alternating pattern of a high-intensity peak next to a lower-intensity peak, the higher intensity peak being closer to the center than the lower-intensity peak, and the q_2/q_1 ratio equal to 1.16. From the FFT of the TEM image of the PS-rich triblock, the ratio of the experimental peak-to-center distances between the second peak to the first peak is 1.14, with the first peak stronger than the second. The best agreement of simulated images with TEM data occurs for models with section thicknesses of about one unit cell ($a = 510$ Å, PS-rich and $a = 530$ Å, PI-rich), in good accord with the measured section thickness. The peaks in the FFT also indexed according to the DG model (Figure 3b).

Four-Fold Projection. Parts a and b of Figure 4 show the TEM images and optical transform of the 4-fold projection of the PS-rich triblock, and parts c and d of Figure 4 show the same for the PI-rich triblock. The TEM images exhibit $p4mm$ symmetry, as do the FFTs for both triblocks.

Two-Fold Projection. The [110] projections of DG have $c2mm$ plane group symmetry. Parts a and b of Figure 5 show the TEM image and optical transform of the PS-rich sample, and parts e and f of Figures 5 show the experimental TEM image and optical transform of the PI-rich sample, all exhibiting $c2mm$ symmetry. In the case of the PI-rich sample there is some skewing of the image and optical transform due to shearing during microtoming. Parts g and h of Figure 5 show the simulated projections and indexed FFTs for a 1-unit-cell-thick DG [110] projection. It should be noted that this projection can also be achieved for unit cell thicknesses ≥ 1 unit cell, due to the existence of the 2-fold screw axes in the DG structure. Both the experimental TEM image and optical transform look qualitatively similar to the [110] TEMsim projection and FFT of the level surface model of DG, respectively. The 2-fold projection is the elucidative cubic symmetry projection for identifying the morphology. The striking resemblance between the experimental 2-fold TEM image and the [110] TEMsim projection of the level surface model of the DG, as well as the good correspondence between the experimental optical transform and the FFT of the TEMsim image, lead us to conclude that the experimentally observed 2-fold images, in both the PI-rich triblock and the PS-rich triblock, are commensurate with the DG morphology.

Thus, from a combination of SAXS, TEM, and geometrical considerations, there is only one suitable space group and interconnected network structure that well satisfies all of our data for each of the two ABA triblocks: the trifunctional double gyroid structure with $Ia\bar{3}d$ symmetry.

Conclusions

Two well-defined triblock copolymers of the ABA type, where A is PS and B is PI, were synthesized using anionic polymerization and chlorosilane chemistry (PI-rich sample). The volume fraction of the minority component is almost the same in both samples (0.36 for the PS-rich and 0.32 for the PI-rich sample). Birefringence measurements showed that both triblocks have isotropic optical properties; TEM images of both samples showed a microphase-separated interconnected/continuous morphology, indicating that the triblocks form cubic, rather than homogeneous, structures. TEM images also showed well-ordered regions exhibiting $p6mm$ in the 6-fold projection, $p4mm$ symmetry in the 4-fold projection, and $c2mm$ symmetry in the 2-fold projection, characteristic of a cubic morphology. SAXS patterns showed two prominent reflections with $q_2/q_1 \approx \sqrt{4}/\sqrt{3}$, indicating eight possible cubic space groups. The observed image symmetries in the three projection directions (the ⟨111⟩, ⟨100⟩, and ⟨$\underline{1}$10⟩) eliminated all but two candidate space groups, $Ia\bar{3}d$ and $Fm\bar{3}m$. Due to the observed interconnectedness of the morphology, consideration was given to the possible topologically connected network structures and the required spatial and geometrical implications. In this manner, the $Fm\bar{3}m$ structure was eliminated, leaving only $Ia\bar{3}d$. Careful examination of the TEM images and computer simulations based on level sets, together with their respective Fourier and optical transforms, lead us to the fact that both samples exhibit the double gyroid structure.

Acknowledgment. We would like to thank Malcolm Capel for his technical assistance at the National Synchrotron Light Source at Brookhaven National Laboratory, Christian Honeker for his cooperation at the beamline and for valuable scientific discussion, John T. Chen for help with the optical bench, and David Hoffman and James Hoffman of the Mathematical Sciences Research Institute, University of California at Berkeley, for development and support of TEMsim. B.J.D. would like to thank the National Science Foundation for providing her fellowship. This project was funded by AFOSR ASSERT No. F49 620-94-1-0357 and ACS PRF No. 30050-AC7.

Note Added to Proof. A recent note by J. H. Laurer et al. (*Macromolecules* **1997**, *30*, 3958), also identifies the double gyroid structure in an isoprene-rich SIS triblock copolymer in which the end blocks form the minority phase.

References and Notes

(1) Aggarwal, S. L. *Polymer* **1976**, *17*, 938. The TEM micrograph showing the novel morphology was taken by J. Beecher. The sample was synthesized by Bi and Fetters (Bi, L-K.; Fetters, L. J. *Macromolecules* **1975**, *8*, 90).
(2) Alward, D. B.; Kinning, D. J.; Thomas, E. L.; Fetters, L. J. *Macromolecules* **1986**, *19*, 215.
(3) Thomas, E. L.; Alward, D. B.; Kinning, D. J.; Martin, D. C.; Handlin, D. L., Jr.; Fetters, L. J. *Macromolecules* **1986**, *19*, 2197.
(4) Thomas, E. L.; Anderson, D. M.; Henkee, C. J.; Hoffman, D. *Nature* **1988**, *334*, 598.
(5) Kinning, D. J.; Thomas, E. L.; Alward, D. B.; Fetters, L. J.; Handlin, D. L. Jr. *Macromolecules* **1986**, *19*, 1288.
(6) Herman, D. S.; Kinning, D. J.; Thomas, E. L.; Fetters, L. J. *Macromolecules* **1987**, *20*, 2940.
(7) Hasegawa, H.; Tanaka, H.; Yamasaki, K.; Hashimoto, T. *Macromolecules* **1987**, *20*, 1651.
(8) Hasegawa, H.; Sumitomo, T.; Hashimoto, T.; Kawai, H. Presented at the 32nd Polymer Symposium of the Society of Polymer Science, Japan, 1983; *Polym. Prepr. Jpn.* **1983**, *32*, 1695.
(9) Longley, W.; McIntosh, T. J. *Nature* **1983**, *303*, 612.
(10) Charvolin, J.; Sadoc, J. F. *J. Phys.* **1987**, *48*, 1559.
(11) Winey, K. I.; Thomas, E. L.; Fetters, L. J. *J. Chem. Phys.* **1991**, *95*, 9367.
(12) Winey, K. I.; Thomas, E. L.; Fetters, L. J. *Macromolecules* **1992**, *25*, 422.
(13) Spontak, R. J.; Smith, S. D.; Ashraf, A. *Macromolecules* **1993**, *26*, 956.
(14) Xie, R.; Yang, B.; Jiang, B. *Macromolecules* **1993**, *26*, 7097.
(15) Mogi, Y.; Kotsuji, H.; Kaneko, Y.; Mori, K.; Matsushita, Y.; Noda, I. *Macromolecules* **1992**, *25*, 5408.
(16) Mogi, Y.; Mori, K.; Matsushita, Y.; Noda, I. *Macromolecules* **1992**, *25*, 5412.
(17) Matsushita, Y.; Chosi, H.; Fujimoto, T.; Nagasawa, M. *Macromolecules* **1980**, *13*, 1053.

(18) Matsushita, Y.; Yamada, K.; Hattori, T.; Fujimoto, T; Sawada, Y; Nagasawa, M.; Matsui, C. *Macromolecules* **1983**, *16*, 10.
(19) Arai, K.; Kotaka, T.; Kitano, Y.; Yoshimura, K. *Macromolecules* **1980**, *13*, 1670.
(20) Kudose, I.; Kotaka, T. *Macromolecules* **1984**, *17*, 2325.
(21) Matsushita, Y.; Tamura, M.; Noda, I. *Macromolecules* **1994**, *27*, 3680.
(22) Mogi, Y.; Nomura, M.; Kotsuji, H.; Ohnishi, K.; Matsushita, Y.; Noda, I. *Macromolecules* **1994**, *27*, 6755.
(23) Gobran, D. Ph.D. Thesis, University of Massachusetts, Amherst, MA, 1990.
(24) Z. Xu, personal communication, 1989.
(25) Hajduk, D. A.; Harper, P. E.; Gruner, S. M.; Honeker, C. C.; Kim, G.; Thomas, E. L.; Fetters, L. J. *Macromolecules* **1994**, *27*, 4063.
(26) Schoen, A. H. *NASA Tech. Rep.* **1970**, No. 05541.
(27) Forster, S.; Khandpur, A. K.; Zhao, J.; Bates, F. S.; Hamley, I. W.; Ryan, A. J.; Bras, W. *Macromolecules* **1994**, *27*, 6922.
(28) Schulz, M.; Bates, F.; Almdal, K.; Mortensen, K. *Phys. Rev. Lett.* **1994**, *73*, 86.
(29) Alward, D. B. Ph.D. Dissertation, University of Massachusetts at Amherst, 1985.
(30) S. Milner, Exxon Research and Engineering, personal communication to E. L. Thomas, 1994.
(31) Hajduk, D. A.; Harper, P. E.; Gruner, S. M.; Honeker, C. C.; Thomas, E. L.; Fetters, L. J. *Macromolecules* **1995**, *28*, 2570.
(32) Tselikas, Y.; Hadjichristidis, N.; Lescanec, R. L.; Honeker, C. C.; Wohlgemuth, M.; Thomas, E. L. *Macromolecules* **1996**, *29*, 3390.
(33) Lambert, C. A.; Radzilowski, L. H.; Thomas, E. L. *Phil. Trans. R. Soc. London A* **1996**, *354*, 2009.
(34) Morton, M.; Fetters, L. J. *Rubber Chem. Technol.* **1975**, *48*, 359.
(35) Iatrou, H.; Hadjichristidis, N. *Macromolecules* **1992**, *25*, 4649.
(36) Iatrou, H.; Hadjichristidis, N. *Macromolecules* **1993**, *26*, 2479.
(37) Capel, M. C.; Smith, G. C.; Yu, B. *Rev. Sci. Instrum.* **1995**, *66*, 2295.
(38) Wohlgemuth, M.; Thomas, E. L. Manuscript in preparation.
(39) http://www.msri.org/Computing/jim/software/temsim/proj/.
(40) Anderson, D.; Bellare, J.; Hoffman, J.; Hoffman, D.; Gunther, J.; Thomas, E. L. *J. Colloid Interface Sci.* **1992**, *148*, 398.
(41) Press, W. H.; Flannery, B. P.; Teukolsky, S. A.; Vetterling, W. T. *Numeral recipes in C: the art of scientific computing*; Cambridge University Press: New York, 1988.
(42) Owens, J. N.; Gancarz, I. S.; Koberstein, J. T.; Russell, T. P. *Macromolecules* **1989**, *22*, 3380.
(43) A reviewer has pointed out to us that W. Fischer and E. Koch (*Z. Kristallogr.* **1987**, *179*, 31) have discovered another possible triply periodic IMDS compatible with the $Ia\bar{3}d$ space group. We are presently unable to determine whether some surface related to the Fischer−Koch S surface would divide space into the volume fractions appropriate to our two triblock samples, as well as produce simulated images that would correspond well with the TEM data. However, since the S surface has a higher genus/unit cell, it will be less likely to occur in physical systems due to an inherently higher surface area at a particular length scale compared to structures based on Schoen's G surface.
(44) Thomas, E. L.; Avgeropoulos A.; Dair B. Manuscript under preparation.

MA970266Z